Histochem Cell Biol (2017) 148:257–272
DOI 10.1007/s00418-017-1568-2

ORIGINAL PAPER

Mapping of estradiol binding sites through receptor micro-autoradiography in the endometrial stroma of early pregnant mice

Telma M. T. Zorn[1] · Rodolfo R. Favaro[1] · Mauricio Soto-Suazo[1,2] · Walter E. Stumpf[1,3]

Accepted: 30 March 2017 / Published online: 17 April 2017

Abstract Estradiol triggers key biological responses in the endometrium, which rely on the presence and levels of its cognate receptors on target cells. Employing the receptor micro-autoradiography (RMAR) technique, we aimed to provide a temporal and spatial map of the functional binding sites for estradiol in the mouse endometrial stroma during early pregnancy. Uterine samples from days 1.5 to 7.5 of pregnancy were collected 1 h after tritiated- (3H-) estradiol administration and prepared for RMAR analysis. Autoradiographic incorporation of 3H-thymidine (after 1-h pulse) was evaluated over the same gestational interval. Combined RMAR with either histochemistry with Dolichus biflorus (DBA) lectin or immunohistochemistry for detection of the desmin further characterized 3H-estradiol binding pattern in uterine Natural Killer (uNK) and decidual cells, respectively. 3H-estradiol binding levels oscillated in the pregnant endometrial stroma between the mesometrial and antimesometrial regions as well as the superficial and deep domains. Although most of the endometrial stromal cells retained the hormone, a sub-population of them, as well as endothelial and uNK cells, were unable to do so. Rises in the levels of 3H-estradiol binding preceded endometrial stromal cell proliferation. 3H-estradiol binding and 3H-thymidine incorporation progressively decreased along the development of the antimesometrial decidua. Endothelial proliferation occurred regardless of 3H-estradiol binding, whereas pericytes proliferation was associated with high levels of hormone binding. Endometrial cell populations autonomously control their levels of 3H-estradiol binding and retention, a process associated with their proliferative competence. Collectively, our results illustrate the intricate regulatory dynamic of nuclear estrogen receptors in the pregnant mouse endometrium.

Keywords Autoradiography · Endometrium · Estrogen · Mouse · Pregnancy

Telma M. T. Zorn and Rodolfo R. Favaro contributed equally.

This article is dedicated to Professor Walter E. Stumpf in memoriam for his valuable contributions to the localization and mechanisms of action of hormones and drugs on tissues, particularly through the development of autoradioautographic approaches, and also for his generosity to share his knowledge with the scientific community.

✉ Telma M. T. Zorn
temtzorn@usp.br

[1] Laboratory of Reproductive and Extracellular Matrix Biology, Department of Cell and Developmental Biology, Institute of Biomedical Sciences, University of São Paulo, Av. Prof. Lineu Prestes 1524; Room 429, São Paulo, SP 05508-000, Brazil

[2] Present Address: Medical School, Finis Terrae University, Santiago, Chile

[3] University of North Carolina at Chapel Hill, Chapel Hill, USA

Introduction

The success of pregnancy depends on a series of biological phenomena leading to the establishment of the maternal–fetal interface. In mice, embryo implantation initiates a cascade of events in the endometrium characterized by the differentiation of endometrial fibroblasts into epithelial-like decidual cells. The decidualized endometrium provides structural and functional support for embryonic growth and placental development (Abrahamsohn and Zorn 1993; Favaro et al. 2014). Decidualization proceeds from the superficial antimesometrial stroma underneath the luminal

epithelium towards the deep stroma situated next to the myometrium, creating regions composed of cells at different stages of differentiation respectively, mature decidual cells, pre-decidual cells, and non-decidualized fibroblast. Later on, decidualization expands to the mesometrial compartment of the uterus (Abrahamsohn 1983; Abrahamsohn and Zorn 1993; Favaro et al. 2014). Mesometrial decidualization induces the influx of uNK cells and engenders the formation and shaping of a wide vascular network in the endometrium, where chorioallantoic placentation takes place. uNK cells contribute to modulate the maternal immune system and to remodel the decidual blood vessels during placentation (Croy et al. 2003; Erlebacher 2014).

Estrogen and progesterone are the master regulators of the endometrial physiology, executing critical roles in the establishment and maintenance of pregnancy (Dey et al. 2004; Adams and DeMayo 2015). Estrogen actions are primarily mediated by estrogen receptors (ERα and ERβ), which operate as ligand-regulated transcriptional factors. Through the classical nuclear signaling pathway, these receptors recognize estrogen-responsive elements (ERE) in the chromatin, regulating gene expression. Furthermore, non-genomic signaling is triggered by membrane-associated receptors, which, for instance, signal through Erk/Mapk and Akt pathways (Binder et al. 2015). Studies with genetically-engineered mice and other approaches revealed that ERα-mediated nuclear signaling predominates in the mouse uterus (Lindberg et al. 2002; Chambliss et al. 2010). Despite of this, ERβ is required for a proper response of the uterine epithelium to estrogen stimulation (Wada-Hiraike et al. 2006).

Estrogen has the ability to regulate the expression of 1000 genes in the mouse uterus, including those coding for transcription factors, growth factors, and cell-matrix interaction components (Hewitt et al. 2003, 2012; Moggs et al. 2004). Accordingly, hormone-dependent changes such as cell proliferation, differentiation, and establishment of specific metabolic patterns occur in all compartments of the uterus. The estrogen-dependent nature of these events has been related to estrogen receptor levels in the cells (Stumpf 1968; Ward et al. 1978; Tibbetts et al. 1998; Oliveira et al. 1995, 1998; Zorn et al. 1995, 2003; Tessier et al. 2000).

Evaluation of steroids receptors in the whole uterus (Sartor 1977; Ward et al. 1978; Moulton and Koenig 1981; De Hertogh et al. 1986) disregards the distribution of these receptors in the different cellular compartments of this organ. Even though informative to discriminate cells expressing steroid receptors, immunohistochemistry and in situ hybridization (Tibbetts et al. 1998; Tan et al. 1999; Tessier et al. 2000) do not provide sufficient resolution to allow the characterization of more subtle variations in hormone receptor density in individual cell types and are unable to provide information regarding the functional status of the receptor. In this sense, autoradiography yields functional data on the binding of the active hormone to its receptor at cellular/sub-cellular level and the regulatory dynamic of this event over time in in vivo models and morphologically preserved tissue preparations (Stumpf and Roth 1966; Stumpf 1971, 2003, 2012; Stumpf et al. 1981).

Using the RMAR technique, we have previously shown during early pregnancy that 3H-estradiol receptor binding is heterogeneously distributed in the epithelium of uterine lumen and glands in a region- and time-related fashion. In addition, 3H-estradiol binding was correlated with epithelial cells proliferation, an essential process for the preparation of the uterus for implantation and conceptus development (Zorn et al. 2003).

In the present study, we aimed to provide a temporal and spatial map of the functional binding sites for 3H-estradiol in the mouse endometrial stromal cells through RMAR. 3H-thymidine incorporation was also analyzed within the same time-frame. Combined autoradiography with either immunohistochemistry for detection of desmin or histochemistry with Dolichus biflorus (DBA) lectin was performed to further characterize the 3H-estradiol binding in cells expressing these markers.

Materials and methods

Animals and tissue preparation

The experiments were approved by the Institute of Biomedical Sciences' Animal Ethics Committee 144/2002 and followed international principles for the use of radioisotopes and for laboratory animal care. The samples examined in this study were originally obtained by Zorn et al. (2003).

Swiss mice aged 3–4 months and ranging in weight from 30 to 37 g were used in the experiments. To know the precise time of pregnancy, females were mated during a 2-h period and then examined for copulation plugs. When plugs were found, this was considered 0-h post coitum. Uterine samples for autoradiographic studies were collected at 1.5, 2.5, 3.5, 4.5, 5.5, 6.5, and 7.5 days of pregnancy from 3 to 4 females each day.

Receptor micro-autoradiography for 3H-estradiol

In each of the aforementioned days of pregnancy, [2,4,6,7,16,17-3H]–Estradiol-17β, specific activity 140 Ci/mMol (New England Nuclear, USA), was dissolved in ethanol-saline 1:10 and injected into the tail vein at a concentration of 0.2 µg per 100 g of body weight. Mice were killed 1 h afterward. Uterine horns were excised and both transversal and longitudinal fragments of 1–2 mm length were placed on tissue holders and freeze-mounted by immersion

into isopentane cooled by liquid nitrogen. Four µm thick frozen sections were cut on a cryostat (Microm 500) and thaw-mounted on emulsion-coated slides (Stumpf 1971, 2003). The mounted slides were stored in a desiccator box at −15 °C for 35, 70, or 100 days. Short-exposure (35 days) autoradiograms were used for silver grain counting and photographic documentation. Long-exposure autoradiograms (70 or 100 days) were used for qualitative and low-magnification surveys. At the end of the exposure, slides were fixed in buffered 2% paraformaldehyde for 1 min, then photographically processed and stained for morphological analysis with methyl green-pyronin. The chemical identity of nuclear radioactivity as being 3H-estradiol has been established in previous experiments (Stumpf 1971; Martel and Psychoyos 1981; Moulton and Koenig 1981).

Quantitative evaluation of autoradiograms

Images were captured and analyzed with the aid of Image-Pro Plus software (Media Cybernetics USA) and a Nikon Eclipse E600 microscope coupled to an Olympus DP-72 camera (Olympus, Japan). Regions of the superficial stroma (close to the luminal epithelium) and deep stroma (near to myometrium) were individually quantitated in transverse sections of mouse uterus from days 1.5 to 4.5 of pregnancy. After decidualization, from days 5.5 to 7.5 of pregnancy, quantification was separately done in the endometrial regions composed by mature decidual cells, pre-decidual cells, and non-decidualized fibroblasts. Quantitation of silver grains was determined in relation to the cell nuclear area. Only nuclei with an area above the mean were selected. For each region analyzed, at least ten nuclei were evaluated per section, at 100× magnification, in three different slides from each of the three mice per day of pregnancy. Statistical analysis was carried out using the GraphPad PRISM software (GraphPad Software, Inc.). Comparisons of 3H-estradiol binding were made between the different endometrial compartments at the same day of pregnancy or between the same compartment from 1 day of pregnancy to the next. Comparisons among means were evaluated by ANOVA followed by Newman–Keuls test and values of $p < 0.05$ were considered statistically significant.

Combined receptor micro-autoradiography and immunohistochemistry or histochemistry

At the end of exposure time, the slides were prepared for immunohistochemical detection of desmin, a marker for decidualized cells (Oliveira et al. 2000) or histochemical detection of DBA lectin to the identification of uNK cells (Paffaro et al. 2003). Samples for the former were fixed in buffered 2% paraformaldehyde for 1 min and samples for the latter were fixed in acetone for 1 min at −20 °C. Fixation was followed by photographic processing of the slides. Following, autoradiograms were treated with 3% H_2O_2 (Merck) in PBS for 30 min to block endogenous peroxidase activity. For immunolocalization of desmin, non-specific reaction was blocked by incubating the sections for 1 h with normal goat serum, diluted 1:1 in PBS containing 10% bovine serum albumin (BSA), followed by incubation with antibody anti-desmin (Sigma) diluted 1:100 in PBS 0.3% Tween 20, overnight at 4 °C. For DBA lectin histochemistry, non-specific reactions were blocked by incubating the sections for 1 h with Super BlockTM solution (Pierce), followed by biotinylated-DBA lectin (Sigma) diluted 1:150 in PBS-0.3% Tween 20, incubated overnight at 4 °C. The sections incubated with antibody against desmin were washed thoroughly with PBS, followed by incubation with goat anti-rabbit IgG conjugated to biotin (Vector), diluted 1:1000 in PBS for 1 h. After extensive rinsing in PBS, all autoradiograms were treated with Vectastain ABC Kit (Vector) for 1 h. The reaction was visualized using 0.03% 3,3′-diaminobenzidine (Sigma) in PBS containing 0.03% H_2O_2. After immunostaining, the sections were stained with Mayer's hematoxylin. Control sections were performed similarly, except by the absence of the primary antibody or the lectin.

Autoradiographic incorporation of 3H-thymidine

3H-Thymidine (New England Nuclear), specific activity 60 Ci/mM, dissolved in distilled water, was injected i.p. 1 µC/g body weight to three mice at the same pregnant periods described above. One hour after the injection, uterine samples were collected and fixed by immersion in Methacarn (methanol, chloroform, glacial acetic acid; 6:3:1) for 3 h, washed, dehydrated, and embedded in Paraplast. Five µm thick sections were placed on glass slides, deparaffinized, hydrated, and then dipped in liquified nuclear emulsion, air-dried, and placed in desiccator boxes for exposure in a refrigerator at 4 °C. After exposure for 60 days, slides were photographically processed, stained with methylgreen-pyronin and coverslipped.

The regional distribution of 3H-thymidine-labeled cells was compared to that of 3H-estradiol-labeled cells, based on a qualitative analysis of the regional labeling patterns without counting individual cells.

Results

Pre-implantation period (days 1.5–4.5 of pregnancy)

3H-Estradiol binding in the antimesometrial endometrial stroma

During the pre-implantation period, from days 1.5 to 4.5 of pregnancy, the lumen of mouse uterus was branched and lined by a simple columnar epithelium. The endometrial stroma underneath the epithelium was formed by loose connective tissue, containing epithelial glands embedded on it. Endometrial fibroblasts were the predominant stromatic cells. A cellular infiltrate consisting especially of neutrophils, eosinophils, and lymphocytes was distributed throughout the stroma. A rich network of blood vessels, especially of the microcirculation, was observed in the endometrium during the pre-implantation period.

On days 1.5, 3.5, and 4.5 (Figs. 1, 2a, b, 4a, b), 3H-estradiol binding was homogeneously distributed in the antimesometrial stromal cells of both superficial and deep stroma. However, on day 2.5 (Figs. 1, 2c, d), the nuclear retention of 3H-estradiol was higher in the superficial than in the deep stroma. Most endometrial stromal cells concentrated 3H-estradiol; however, some of them were unable to retain the hormone during all the pre-implantation period (Figs. 2a–d, 4a–d). Pericytes showed the highest concentration of 3H-estradiol in the endometrial stromal compartment (Fig. 3). Quantification of silver grains on these cells revealed that they bind around 40–50% more 3H-estradiol than other stromal cells. In

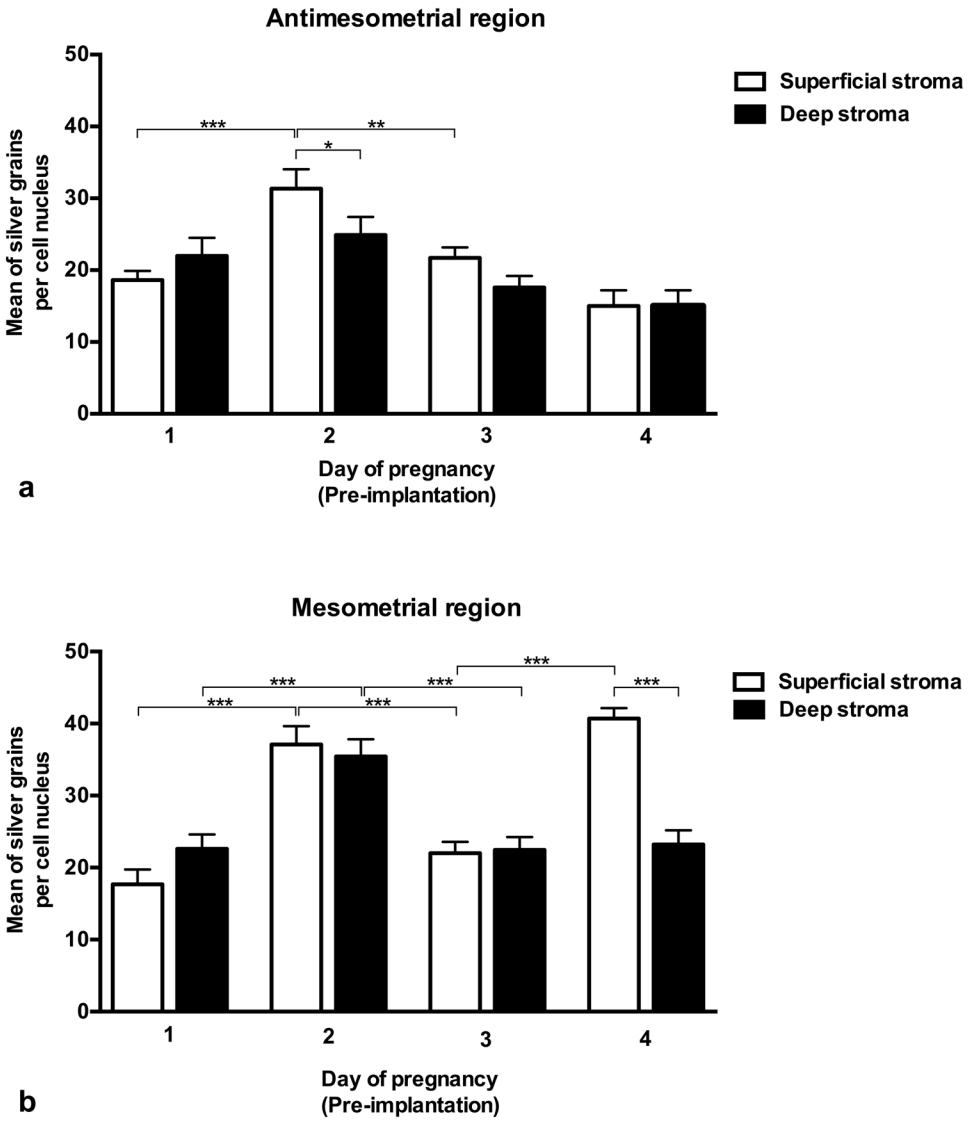

Fig. 1 Quantitative evaluation of 3H-estradiol binding in the antimesometrial (**a**) and mesometrial endometrial stroma (**b**) of mice from days 1.5 to 4.5 of pregnancy. Silver grain counts over cell nuclei were evaluated in three animals per time period and the mean (±SEM) of over 30 cells per stromal region per animal. *$p \leq 0.05$; **$p \leq 0.01$; ***$p \leq 0.001$

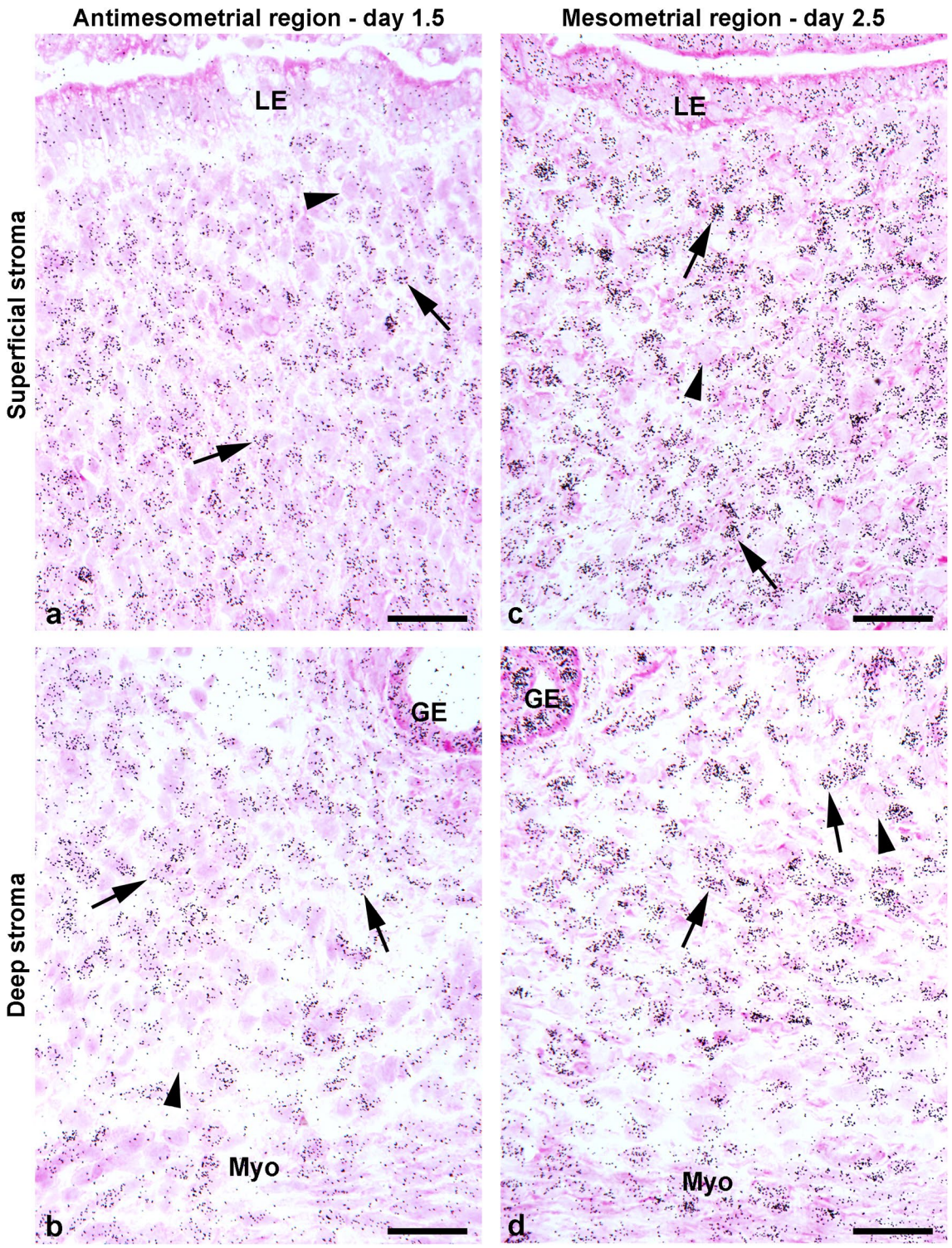

Fig. 2 Receptor micro-autoradiographic mapping of 3H-estradiol binding in the antimesometrial endometrial stroma of mice on days 1.5 and 2.5 of pregnancy. **a, b** On day 1.5, 3H-estradiol binding is homogeneously distributed on cells of both superficial stroma and deep stroma. Although most stromal cells bind 3H-estradiol (*arrows*), some are unable to retain the hormone (*arrowheads*). **c, d** Note that on day 2.5, the concentration of silver grains is higher in the superficial stroma than in the deep stroma. Methyl green-pyronin stains the cell nucleus *light blue* and the cytoplasm *red. LE* luminal epithelium, *GE* glandular epithelium, *Myo* myometrium. *Scale bar* 30 µm

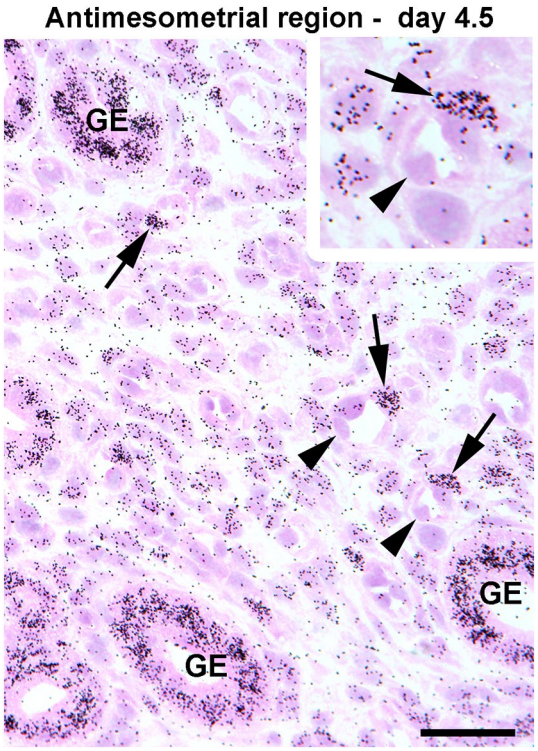

Fig. 3 Receptor micro-autoradiographic mapping of 3H-estradiol binding in the blood vessels of the antimesometrial endometrial stroma of mice on day 3.5 of pregnancy. While pericytes (*arrows*) concentrate high amounts of 3H-estradiol, endothelial cells (*arrowheads*) do not retain the hormone. The *insert* shows in more detail a blood vessel containing a strongly labeled pericyte. *LE* luminal epithelium, *GE* Glandular epithelium. Methyl green-pyronin stains the cell nucleus *light blue* and the cytoplasm *red. Scale bar* 30 µm

contrast, no retention of the hormone was observed in endometrial endothelial cells (Fig. 3).

3H-Estradiol binding in the mesometrial endometrial stroma

Similar to observed in the antimesometrial region, the nuclear concentration of 3H-estradiol in the mesometrial region oscillated during the pre-implantation period. Quantitative analysis showed an increase of nuclear labeling in endometrial stromal cells on day 2.5, compared to the previous day of pregnancy, which decreased again on day 3.5. These changes occurred uniformly in both superficial and deep endometrial stroma (Fig. 1). Contrarily, 3H-estradiol binding increased on day 4.5 exclusively in the superficial stroma (Figs. 1, 4c, d). In addition, a single layer of stromal cells localized immediately underneath the luminal epithelium presented a strong retention of 3H-estradiol (Fig. 4c).

Post-implantation period (days 5.5–7.5 of pregnancy)

3H-Estradiol binding in the antimesometrial endometrial stroma

The first decidual cells were observed around the implanting embryo on day 5.5 of pregnancy. Surrounding them, there were pre-decidual cells, whose phenotype is intermediated between mature decidual cells and endometrial fibroblasts. The most peripheral stroma, close to the myometrium, was formed by non-decidualized fibroblasts. A weak binding to 3H-estradiol was detected in the antimesometrial stromal cells on day 5.5 (Fig. 5).

Decidualization expanded on the following days (6.5–7.5). Desmin-positive decidual cells occupied most of the antimesometrial portion in the endometrium. These cells were large, polygonal, and closely apposed to each other. Qualitative and quantitative evaluation showed that the 3H-estradiol binding in the endometrial stroma increased from days 5.5 to 6.5 (Figs. 5, 6a-c). A gradient of binding was observed according to the region of the stroma and the correspondent degree of decidualization of its cells. Very weak/absent 3H-estradiol radioactive signals were detected in mature/involuting decidual cells surrounding the embryo, followed by weak/moderate signals in decidual cells far from the embryo and an intense labeling in pre-decidual cells and non-decidualized stromal cells (Figs. 5, 6a–c). 3H-estradiol retention decreased on pre-decidual cells from days 6.5 to 7.5 (Fig. 5). Scattered between mature decidual cells in the antimesometrial region, there were small cells strongly labeled with 3H-estradiol, but immunonegative for the decidual marker desmin (Fig. 6a-insert).

No 3H-estradiol nuclear concentration was observed in the antimesometrial endothelial cells as well as in trophoblast and embryonic cells.

3H-Estradiol binding in the mesometrial endometrial stroma

The first signs of decidualization in the mesometrial endometrium were observed on day 6.5 of pregnancy. Mesometrial decidual cells were smaller and not close apposed as in the antimesometrial endometrium.

Although 3H-estradiol binding on days 5.5 to 7.5 was similar between the superficial and deep stroma, a general reduction in the levels of binding was detected from days 6.5 to 7.5 (Fig. 5). The number of the sinusoid or lacunae blood vessels in the mesometrial endometrium increased remarkably on day 7.5. Nevertheless, mesometrial endothelial cells showed no binding to 3H-estradiol during the post-implantation period (Fig. 7a). Based on 3H-estradiol retention patterns allied to the histochemical identification

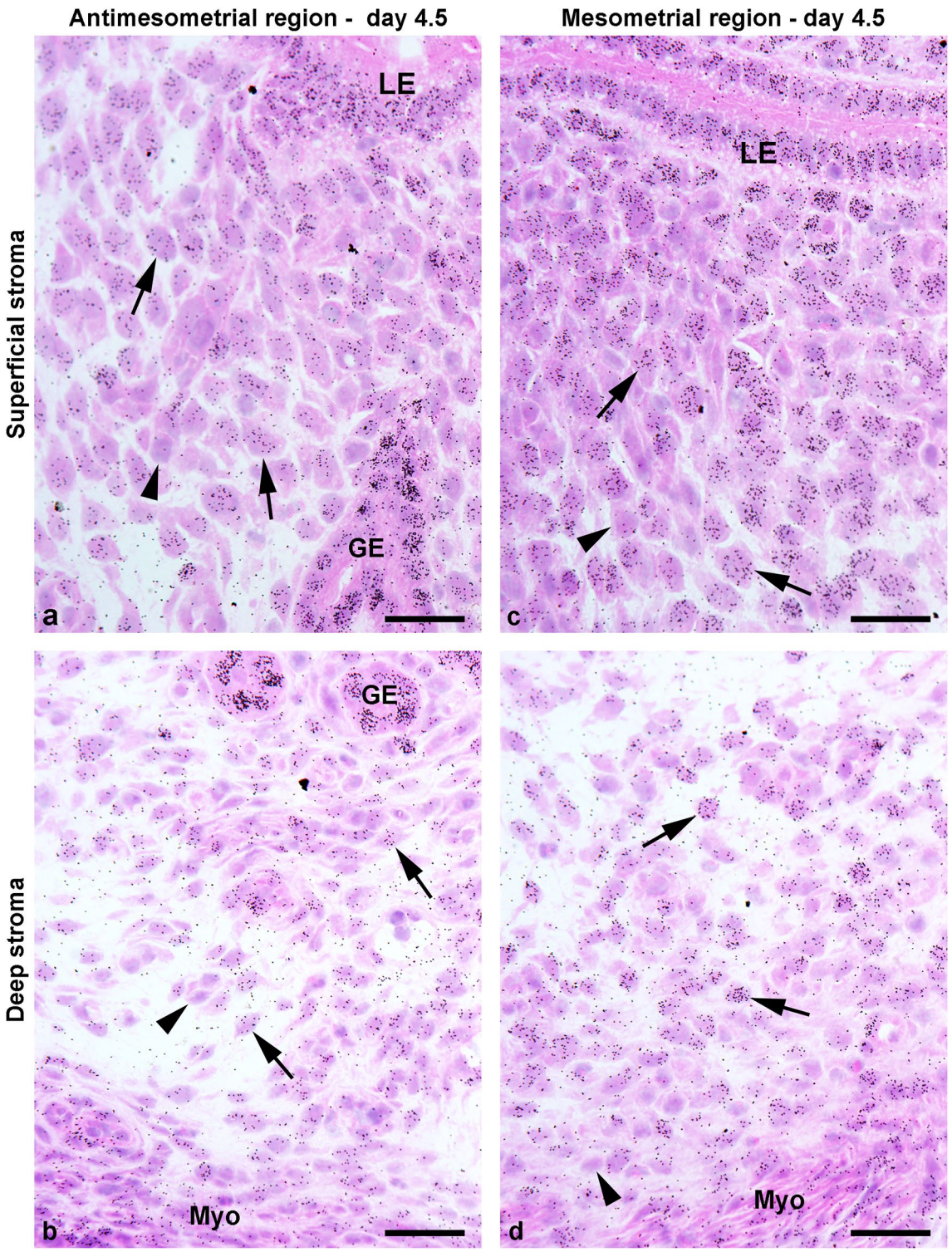

Fig. 4 Receptor micro-autoradiographic mapping of 3H-estradiol binding in the endometrial stroma of mice on day 4.5 pregnancy. **a, b** In the antimesometrial region, silver grains are homogeneously distributed between cells (*arrows*) of the superficial and deep stroma. Cells without 3H-estradiol retention can also be observed (*arrowheads*). **c, d** In contrast, 3H-estradiol binding density in the mesometrial region is higher on cells (*arrows*) of the superficial stroma than of the deep stroma. Observe a single layer of strongly labeled stromal cells underneath the luminal epithelium (LE) and cells without 3H-estradiol retention (*arrowheads*). Methyl green-pyronin stains the cell nucleus *light blue* and the cytoplasm *red. GE* glandular epithelium, *Myo* myometrium. *Scale bar* 30 µm

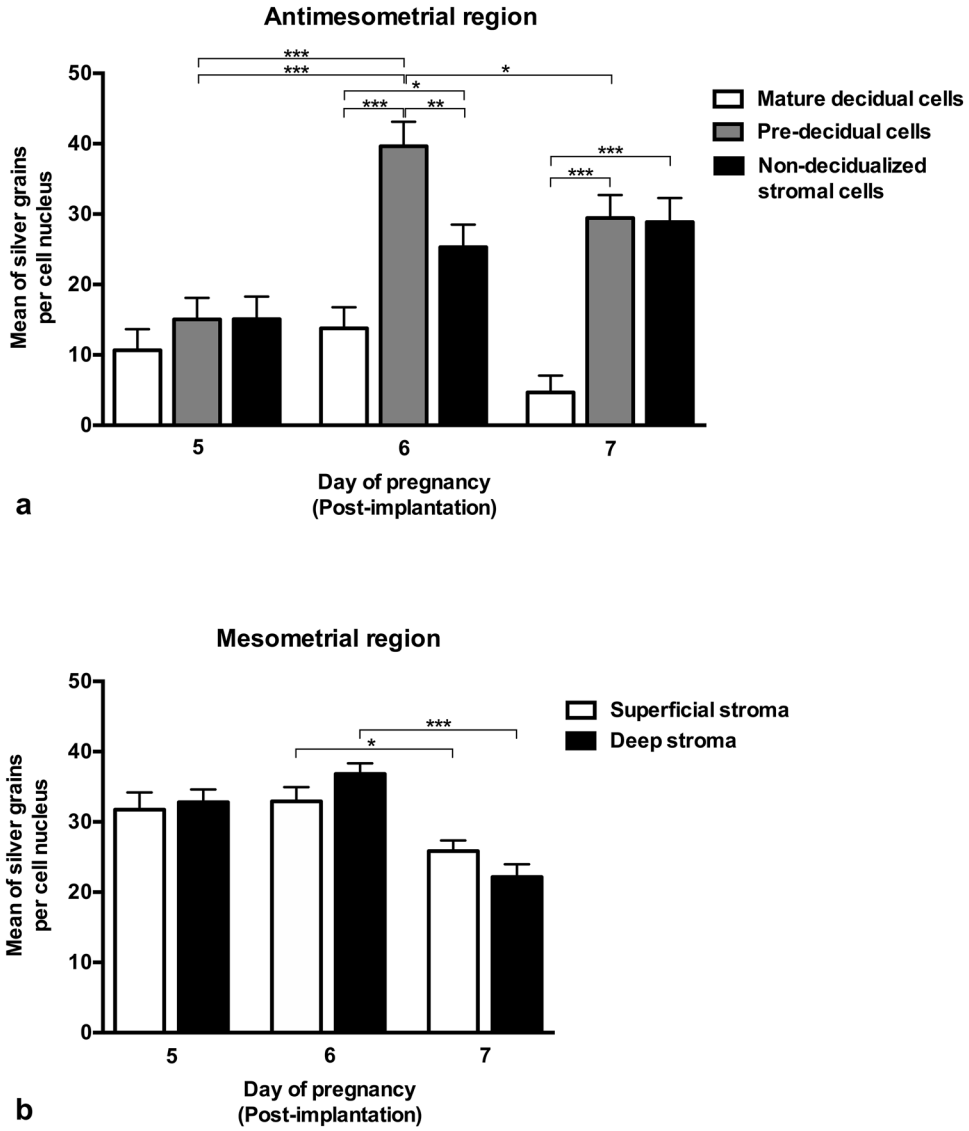

Fig. 5 Quantitative evaluation of 3H-estradiol binding in the antimesometrial (**a**) and mesometrial endometrial stroma (**b**) of mice from days 5.5 to 7.5 of pregnancy. Silver grain counts over cell nuclei were evaluated in three animals per time period and the mean (±SEM) of over 30 cells per stromal region per animal. *SS* superficial stroma, *DS* deep stroma, *MDC* mature decidual cells, *PDC* pre-decidual cells, *NDS* non-decidualized stromal cells. *$p \leq 0.05$; **$p \leq 0.01$; ***$p \leq 0.001$

of DBA lectin (Fig. 7b), three main populations of cells were recognized in the endometrial stroma of the mesometrial region: (1) stromal/decidual cells; (2) uNK cells; and (3) vascular precursors/endothelial cells. Mesometrial stromal/decidual cells showed high 3H-estradiol retention, whereas part of the cells devoid of 3H-estradiol binding were histochemically labeled by DBA lectin and, thus, identified as uNK cells. Predominantly on day 6.5, a population of DBA lectin-negative cells, probably vascular precursors, were organized in cord-like structures and did not bind 3H-estradiol (Fig. 7b).

3H-Thymidine incorporation in the endometrium

Different from the luminal and glandular epithelial cells, endometrial stromal cells did not incorporate 3H-thymidine on days 1.5 and 2.5 of pregnancy (Fig. 8a). On day 3.5 (Fig. 8b, d), this proliferative profile shifted from the epithelium to the stroma. Endometrial stromal cells incorporated the radiolabeled precursor in both mesometrial and antimesometrial regions, predominantly in the superficial stroma of the latter. Pericytes and a few endothelial cells also proliferated all over the endometrium. On the next day (Fig. 8c, e), very few stromal cells incorporated thymidine. In contrast, pericytes and endothelial cells proliferated intensively.

After the beginning of decidualization in the antimesometrial endometrial stroma, on days 5.5 and 6.5 (Figs. 9a, 10a), pre-decidual cells and non-decidualized fibroblasts showed high levels of 3H-thymidine incorporation, whereas radioactive signals were low or absent in mature and involuting decidual cells. On day 7.5, 3H-thymidine incorporation occurred only in a limited number of pre-decidual cells. The proliferation of pericytes and

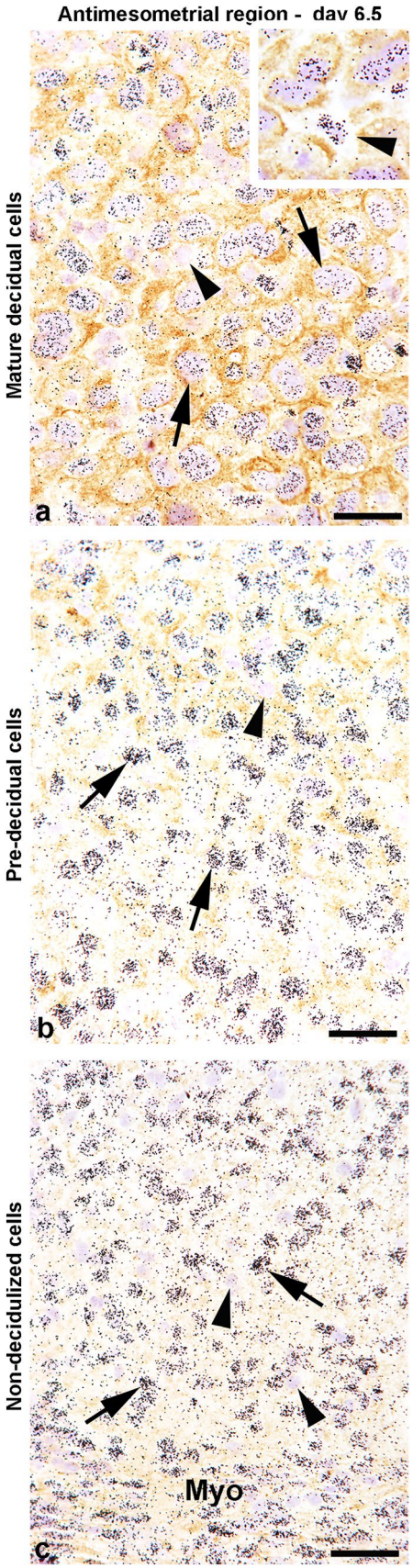

Fig. 6 Receptor micro-autoradiographic mapping of 3H-estradiol binding combined with immunohistochemistry for desmin in the antimesometrial decidua of mice on day 6.5 of pregnancy. 3H-estradiol concentration in the endometrial stroma varies according to the region of the endometrium. **a** Lowest levels of 3H-estradiol binding are observed in mature decidual cells (*arrows*). **b** Pre-decidual cells (*arrows*) show the highest levels of 3H-estradiol binding, whereas **c** non-decidualized stromal cells (*arrows*) present an intermediated degree of binding between mature decidual cells and pre-decidual cells. Cells without 3H-estradiol binding (*arrows*) are present in all regions of the endometrium. The insert highlights a desmin-negative cell (*arrowhead*) with high estradiol binding. Methyl green stains the cell nucleus *light blue*. *Myo* myometrium; *Scale bar* 30 µm

endothelial cells in the antimesometrial region progressively decreased from days 5.5 (Fig. 9a) to 7.5. Endothelial cells present on fully decidualized areas from the antimesometrial endometrium showed no thymidine incorporation.

On the mesometrial region, 3H-thymidine incorporation on days 3.5 and 5.5 (Fig. 9b) was found in endometrial stromal cells, particularly from the superficial stroma, pericytes, and endothelial cells. Similar to what was observed in the antimesometrial endometrium, only pericytes and endothelial cells proliferated on day 4.5 in the mesometrial endometrium. On day 6.5 (Fig. 10b), 3H-thymidine incorporation was detected in the transition between the antimesometrial and mesometrial regions as well as in the mesometrial region. On the following day, cell proliferation was predominantly detected on the mesometrial pole of the endometrium.

Endothelial cells of the mesometrial region proliferated on days 5.5 and 6.5 (Figs. 9b, 10b). On day 7.5, proliferation of endothelial cells from blood vessels at the transition between the antimesometrial and mesometrial decidua was low or absent (Fig. 10c). Differently, endothelial cells of blood vessels facing the mesometrial region were actively proliferating (Fig. 10d).

Discussion

Due to the central role of estrogen in uterine physiology and disease, we advocate that all efforts should be made to enlarge our knowledge on the localization, distribution, and dynamics of estrogen receptors in this organ. In this regard, RMAR provides cellular/sub-cellular resolution and high sensitivity for the identification of *in vivo* hormone binding sites in target tissues. After injection of 3H-estradiol, functional sites of uptake and binding in the cells can be not simply identified but also quantified. The localized radioactivity reflects the acting hormone that binds to its receptors with different affinities and capacities related to tissue-specific functions (Stumpf 1971, 2003, 2012; Zorn et al. 2003).

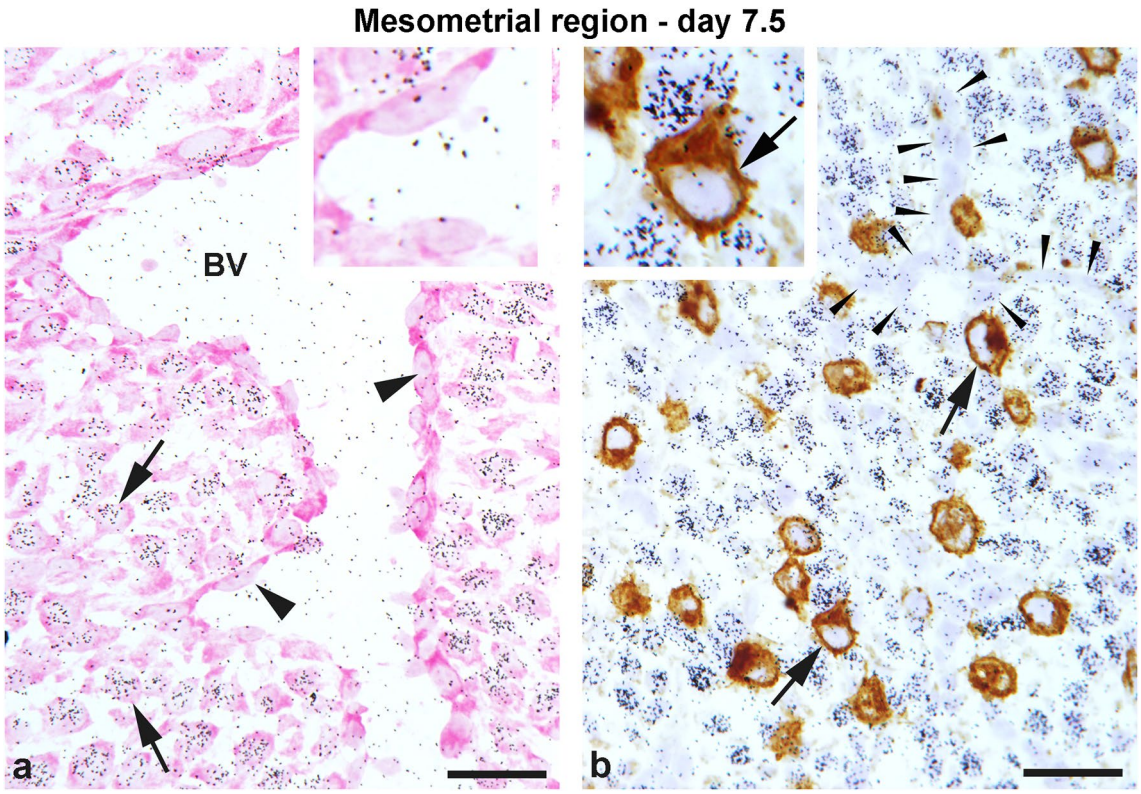

Fig. 7 **a** Receptor micro-autoradiographic mapping of 3H-estradiol binding in the blood vessels of the mesometrial decidua of mice on the 7.5 day of pregnancy. Different from stromal cells (*arrow*), endothelial cells lining the wide blood vessels (BV) of the mesometrial decidua do not retain 3H-estradiol. Methyl green-pyronin stains the cell nucleus *light blue* and the cytoplasm *red. Scale bar* 30 µm. **b** Receptor micro-autoradiographic mapping of 3H-estradiol binding combined with histochemistry to DBA lectin in the mesometrial decidua of mice on day 7.5 of pregnancy. DBA-positive uNK cells (*arrows*) show no biding to 3H-estradiol. The *insert* presents a higher magnification of these cells. Cells negative for DBA lectin and without 3H-binding (*arrowheads*) are organized into cord-like structures in the mesometrial decidua. Methyl green stains the cell nucleus *light blue*. *Scale bar* 30 µm

ERα is widely expressed in the uterine tissues, including the luminal and glandular epithelia, endometrial fibroblasts, and myometrium, whereas ERβ is weakly expressed in these same tissues (Tan et al. 1999; Binder et al. 2015). Data obtained in the present study by RMAR concerning the distribution and localization of 3H-estradiol binding in the mouse endometrial cells is in agreement with results obtained by in situ hybridization and immunohistochemistry for estrogen receptors (Tibbetts et al. 1998; Tan et al. 1999; Tessier et al. 2000). Nevertheless, RMAR allowed the identification of unrecognized facets of estrogen receptor dynamics in the mouse endometrial stroma during early pregnancy.

Our data on 3H-estradiol binding, in addition to identifying distinct populations of cells, demonstrated the patterns of compartmentalization existing in the mouse endometrium into mesometrial and antimesometrial regions as well as the sub-compartmentalization of the stroma from these regions into superficial and deep domains. Remarkably, 3H-estradiol binding oscillated independently on these endometrial compartments, sub-compartments, and their cells populations. In the human endometrium, estrogen and progesterone receptors are also differently expressed in the basal and functional layers (Coppens et al. 1993; Critchley et al. 2001). These results reinforce previous studies from our group showing that the mouse endometrium presents a compartmentalization similar to that of the human endometrium (Oliveira et al. 1995, 1998; Zorn et al. 1995; Greca et al. 1998; Salgado et al. 2009a, b, 2011, 2013; Favaro et al. 2014). While the superficial stroma (functional layer in humans) commits with decidualization, the deep stroma (basal layer) remains undifferentiated and contributes to reconstruct the endometrium after pregnancy (Abrahamsohn 1983; Kleinfeld and O'Shea 1983; Favaro et al. 2014; Cao et al. 2015).

A small fraction of the endometrial stem cells expresses ERα in mice, and the treatment of ovarectomized females with estrogen stimulates the proliferation of the stem cell population (Chan and Gargett 2006). Our results support the lack of 3H-estradiol binding in part of the endometrial stromal cells during early pregnancy; however, we were unable to specifically discriminate stem cells. Lack

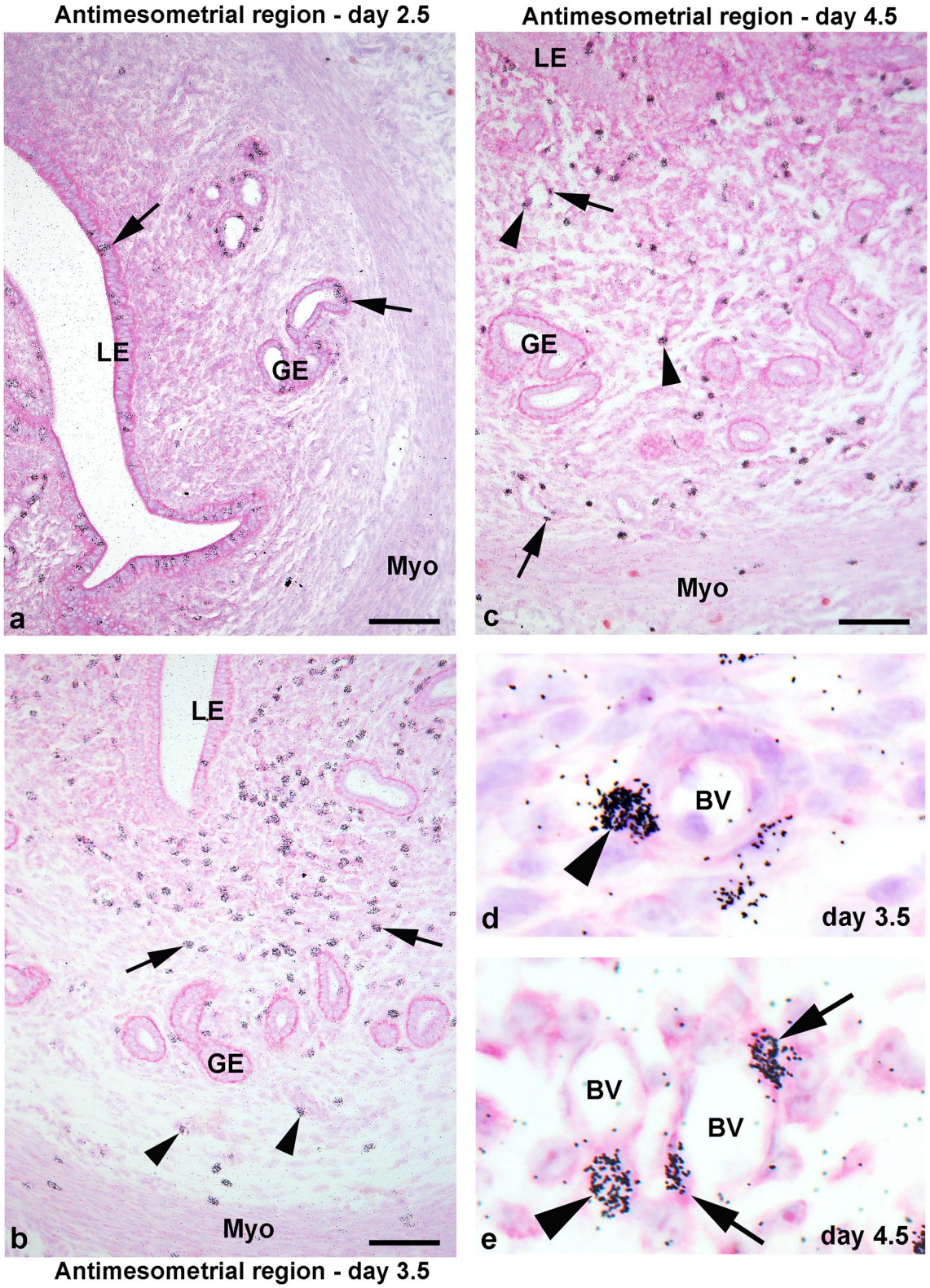

Fig. 8 Autoradiographic analysis of 3H-thymidine incorporation in the antimesometrial endometrium of mice on days 2.5 (**a**), 3.5 (**b**), and 4.5 (**c**) of pregnancy. **a** On day 2.5, proliferating cells (*arrows*) can be observed in both luminal (LE) and glandular epithelia (GE). **b, d** On day 3.5, the epithelia are not dividing. In turn, proliferating cells (*arrows*) are observed in the endometrial stroma, especially at the superficial stroma. Pericytes (*arrowheads*), observed in detail on **(d)**, also proliferate on this day of pregnancy. (**c, e**) Only pericytes (*arrowheads*) and endothelial cells (*arrows*) proliferate in the endometrium on day 4.5, as highlighted in (**e**). Methyl green-pyronin stains the cell nucleus *light blue* and the cytoplasm *red*. *Myo* myometrium. *Scale bar* 50 µm

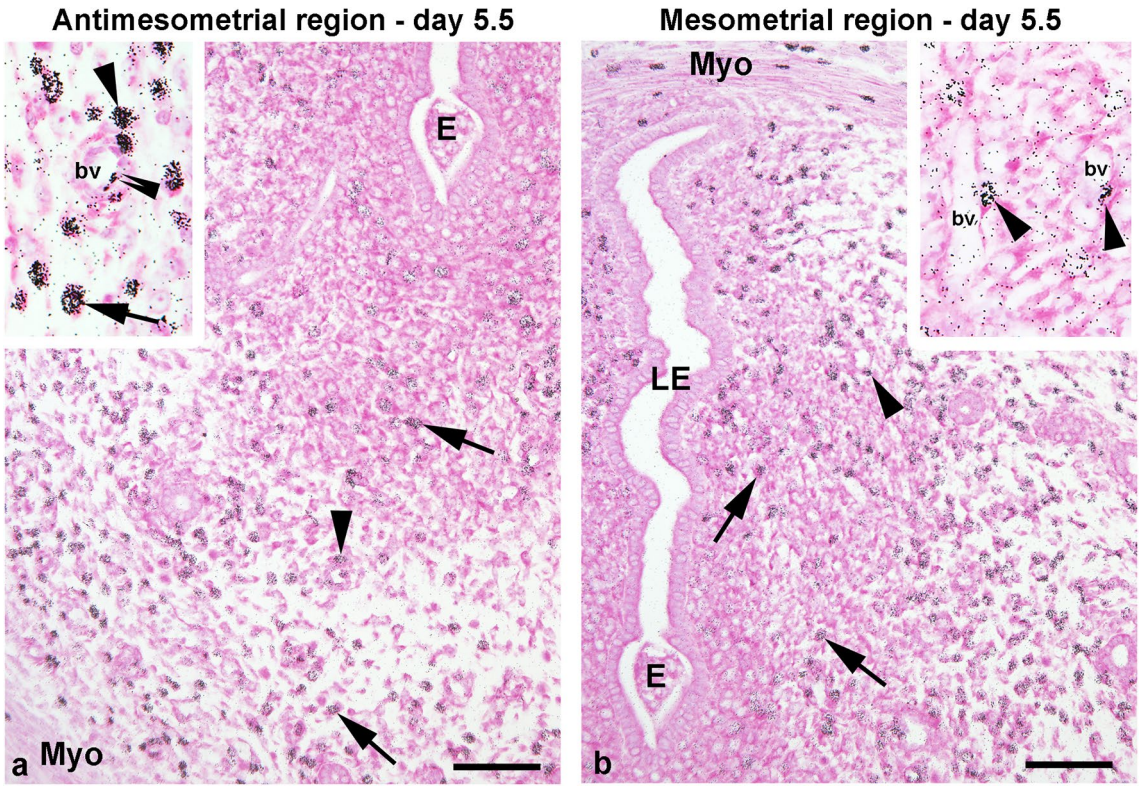

Fig. 9 Autoradiographic analysis of 3H-thymidine incorporation in the antimesometrial (**a**) and mesometrial endometrium (**b**) of mice on day 5.5 of pregnancy. **a** Stromal cells (*arrows*) as well as pericytes (*arrowheads*) and endothelial cells (*double arrowhead*) proliferate on this day throughout the antimesometrial endometrium, as highlighted in the *insert*. **b** On the mesometrial endometrium, the incorporation of thymidine is present in stromal (*arrows*) and endothelial cells (*arrowheads*). The *insert* portraits the incorporation of thymidine into mesometrial endothelial cells (*arrowheads*). Methyl green-pyronin stains the cell nucleus *light blue* and the cytoplasm *red*. *E* embryo; *Scale bar* 50 µm

of estrogen receptors on part of the endometrial stem cells may prevent them to respond all at once to the hormone, what could exhaust their population. This strategy may contribute to the maintenance of a reservoir of non-differentiated stromal cells in the mouse endometrium, even when exposed to high levels of estrogen.

Marked structural and functional adaptations take place in the endometrium during early pregnancy. A particular and sequential pattern of cell proliferation, differentiation, polyploidy, and death occurs in the endometrium in preparation for and during decidualization (Abrahamsohn 1983; Abrahamsohn and Zorn 1993; Favaro et al. 2014). Proliferation of endometrial fibroblasts from the antimesometrial and mesometrial endometrium, respectively, on days 3.5 and 5.5, was preceded by rises in 3H-estradiol binding on these compartments. The absence of endometrial fibroblasts proliferation on day 4.5 of pregnancy may be related to their differentiation and capacitation to respond to the decidual stimulus, as part of the implantation window (Ma et al. 2003).

Fig. 10 Autoradiographic analysis of 3H-thymidine incorporation in the antimesometrial (**a**) and mesometrial endometrium (**b**) of mice on day 6.5 of pregnancy and mesometrial endometrium on day 7.5 of pregnancy (**c**, **d**). **a** Decreasing gradient of 3H-thymidine incorporation (*arrows*) is present from non-decidualized stromal cells (NDS) and pre-decidual cells (PDC) towards mature decidual cells (MDC). **b** At the mesometrial endometrial stroma, a great number of stromal cells (*arrows*) and endothelial cells (*arrowheads*) incorporate 3H-thymidine on day 6.5 of pregnancy. **c** On day 7.5, endothelial cells (*arrowheads*) from blood vessels of the mesometrial pole show intense proliferation. **d** In contrast, endothelial cells (*arrowheads*) close to the antimesometrial region present low levels of proliferation. Methyl green-pyronin stains the cell nucleus *light blue* and the cytoplasm *red*. *BV* blood vessels, *Myo* myometrium. *Scale bar* 50 µm

A parallel and progressive decreasing of 3H-estradiol binding and 3H-thymidine incorporation occurred along the development of the antimesometrial decidua. While endometrial fibroblasts and pre-decidual cells concentrated high amounts of 3H-estradiol, mature decidual cells retained low amounts and involuting decidual cells lost the ability to concentrate the hormone, as a consequence of changes in the expression of estrogen receptor protein, as previously evidenced by immunohistochemistry (Tan et al.

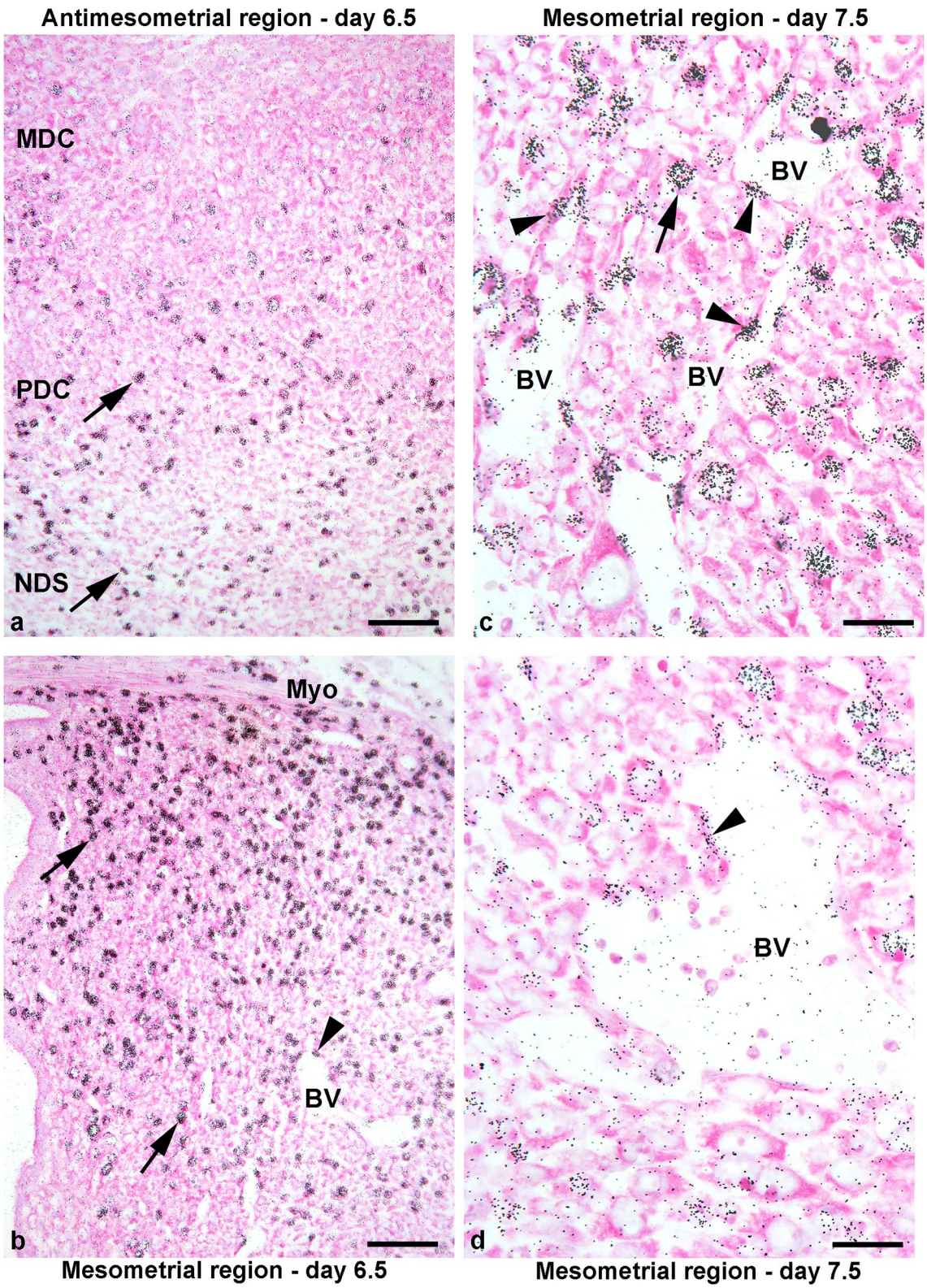

1999). The mesometrial decidua develops somewhat later than the antimesometrial decidua and contributes to the formation of the chorioallantoic placenta (Abrahamsohn and Zorn 1993; Favaro et al. 2014). Accordingly, stromal cells of the mesometrial compartment retained 3H-estradiol and actively proliferated during the post-implantation period. Results from the literature indicate that thymidine incorporation observed in this compartment were originated from

the proliferation of stromal fibroblasts and decidual cells (Gao et al. 2015) as well as uNK cells (Croy et al. 2003; Herington and Bany 2007). Taken together, these results highlight the relevance of estradiol binding for endometrial proliferation and decidualization.

Apparently, the embryo does not exert noticeable influences in the 3H-estradiol binding in the decidualized endometrium. Similar patterns of hormonal retention were detected when the decidua of normal pregnancy was compared with the embryo-free artificially-induced deciduoma (data not shown).

Estrogen alone or followed administrations of estrogen and progesterone stimulate angiogenesis in the endometrium of ovariectomized mice (Heryanto and Rogers 2002). Estrogen regulates several angiogenic factors in the mouse uterus, including Angiopoietin-2 and VEGF (Walter et al. 2010; Guo et al. 2012). Furthermore, similar to human decidual cells (Gibson et al. 2013), mouse decidual cells are able to synthesize estrogen during pregnancy, which is critical for endometrial angiogenesis. The pharmacological inhibition of this process impairs decidualization and angiogenesis through disturbed expression of angiogenic factors (Das et al. 2009).

Pericytes take an active role in the angiogenic processes (Betsholtz et al. 2005), and their multiplication preceding embryo implantation harmonizes with the increasing of endometrial blood vessels in this period (Walter et al. 2005). While the proliferation of pericytes was associated with a high binding of 3H-estradiol, endothelial cells from all compartments of the endometrium, and gestational age investigated, proliferated regardless of 3H-estradiol nuclear binding. The expression of estrogen receptors, particularly ERβ, has been reported in endothelial cells of the human and rhesus monkey endometrium during the reproductive cycle and early pregnancy (Perrot-Applanat et al. 1994; Critchley et al. 2001). The genomic effects of estrogen on human endothelial cells are mediated by ERβ via tethered interactions with the transcription factor Sp1, in an ERE-independent manner (Greaves et al. 2013). The present data, obtained through RMAR, supports the lack of nuclear binding sites for 3H-estradiol on mouse endometrial endothelial cells in vivo, pointing out a divergence in the action of estrogen on endometrial endothelial cells of humans and mice. Nevertheless, our experimental setting cannot rule out the existence of estrogen receptors on mouse endometrial endothelial cells, where they may signal via rapid, membrane-initiated non-genomic pathways (Wu et al. 2011). Collectively, evidence indicates that some actions of estrogen in the endometrial blood vessel cells of mice are directly activated by this hormone on target cells, whereas other effects are paracrinally mediated by estrogen-responsive endometrial cells, such as decidual cells (Das et al. 2009).

Through combined RMAR and histochemistry, we demonstrated that DBA lectin-positive uNK cells were unable to retain 3H-estradiol. This is consistent with the lack of estrogen receptors (ERα and ERβ) in mouse uNK cells (Borzychowski et al. 2003) that, in turn, diverge from their human counterparts, which are responsive to estrogen through the expression of ERβ (Henderson et al. 2003; Gibson et al. 2015). A population of small cells strongly binding 3H-estradiol was particularly evident in the decidualized endometrial stroma on days 6.5 and 7.5 of pregnancy. Combined autoradiography and immunohistochemistry demonstrated that these cells were not decidual cells, due to the lack of immunoreaction for desmin (Oliveira et al. 2000). Further experiments are needed to determine the identity of these cells.

In summary, endometrial cell populations independently regulate their levels of 3H-estradiol retention and binding, a process associated with their proliferative competence. 3H-estradiol binding patterns revealed the intrinsic compartmentalization of the mouse endometrium into mesometrial and antimesometrial regions as well as their stroma into superficial and deep domains. Data presented in this study disclose a complex regulatory dynamic of estradiol binding in the pregnant endometrial stroma of mice, which may be related to the diversity of functions played by this hormone in the uterine environment.

Acknowledgements The authors would like to thank Mrs. Cleusa Pellegrini for her enormous and precious support in the preparation of the samples for autoradiographic analysis. Grants (99/00098-1 and 99/00097-5; TMTZ) were provided by São Paulo Research Foundation-FAPESP. Fellowships were provided by FAPESP (11/22429-3; RRF) and by Coordination for the Improvement of Higher Education Personnel—CAPES (20131525; RRF).

Compliance with ethical standards

Conflict of interest The authors declare that they have no conflict of interest.

References

Abrahamsohn PA (1983) Ultrastructural study of the mouse antimesometrial decidua. Anat Embryol 166(2):263–274

Abrahamsohn PA, Zorn TMT (1993) Implantation and decidualization in rodents. J Exp Zool 266:603–628

Adams NR, DeMayo FJ (2015) The role of steroid hormone receptors in the establishment of pregnancy in rodents. Adv Anat Embryol Cell Biol 216:27–49

Betsholtz C, Limdblom P, Gerharddt H (2005) Role of pericytes in vascular morphogenesis. In: Clauss M, Breier G (eds) Mechanisms of angiogenesis. Birkhäuser Verlag, Basel, pp 115–125

Binder AK, Winuthayanon W, Hewitt SC, Couse JF, Korach KS (2015) Steroid receptors in the uterus and ovary. In: Plant TM, Zeleznik AJ (eds) Knobil and Neill's physiology of reproduction, 4th edn. Elsevier, San Francisco, pp 1099–1193

Borzychowski AM, Chantakru S, Minhas K, Paffaro VA, Yamada AT, He H, Korach KS, Croy BA (2003) Functional analysis of murine uterine natural killer cells genetically devoid of oestrogen receptors. Placenta 24(4):403–4 11

Cao M, Chan RW, Yeung WS (2015) Label-retaining stromal cells in mouse endometrium awaken for expansion and repair after parturition. Stem Cells Dev 24(6):768–780

Chambliss KL, Wu Q, Oltmann S et al (2010) Non-nuclear estrogen receptor alpha signaling promotes cardiovascular protection but not uterine or breast cancer growth in mice. J Clin Invest 120(7):2319–2330

Chan RW, Gargett CE (2006) Identification of label-retaining cells in mouse endometrium. Stem Cells 24(6):1529–1538

Coppens MT, Dhont MA, De Boever JG, Serreyn RF, Vandekerckhove DA, Roels HJ (1993) The distribution of oestrogen and progesterone receptors in the human endometrial basal and functional layer during the normal menstrual cycle. An immunocytoche mical study. Histochemistry 99(2):121–126

Critchley HO, Brenner RM, Henderson TA, Williams K, Nayak NR, Slayden OD, Miller MR, Saunders PT (2001) Estrogen receptor β, but not estrogen receptor α, is present in the vascular endothelium of the human and nonhuman primate endometrium. J Clin Endocrinol Metab 86:1370–1378

Croy AB, He H, Esadeg S et al (2003) Uterine natural killer cells: insights into their cellular and molecular biology from mouse modelling. Reproduction 126:149–160

Das A, Mantena SR, Kannan A, Evans DB, Bagchi MK, Bagchi IC (2009) De novo synthesis of estrogen in pregnant uterus is critical for stromal decidualization and angiogenesis. Proc Natl Acad Sci USA 106(30):12542–12547

De Hertogh R, Ekka E, Vanderheyden I, Glorieux B (1986) Estrogen and progestogen receptors in the implantation sites and interembryonic segments of rat uterus endometrium and myometrium. Endocrinology 119:680–684

De M, Choudhuri R, Wood GW (1991) Determination of the number and distribution of macrophages, lymphocytes and granulocytes in the mouse uterus from mating through implantation. J Leuk Biol 50:252–262

Dey SK, Lim H, Das SK, Reese J, Paria BC, Daikoku T, Wang H (2004) Molecular cues to implantation. Endocr Rev 25(3):341–373

Erlebacher A (2014) Leukocyte Population Dynamics and Functions at the Maternal–Fetal Interface. In: Croy A, Yamada AT, DeMayo F, Adamson S (eds) The guide to investigation of mouse pregnancy, 1th edn. Elsevier, Boston, pp 227–242

Favaro R, Abrahamsohn P, Zorn T (2014) Decidualization and endometrial extracellular matrix remodeling. In: Croy A, Yamada AT, DeMayo F, Adamson S (eds) The guide to investigation of mouse pregnancy, 1th edn. Elsevier, Boston, pp 125–142

Gao F, Bian F, Ma X, Kalinichenko VV, Das SK (2015) Control of regional decidualization in implantation: Role of FoxM1 downstream of Hoxa10 and cyclin D3. Sci Rep 5:13863. doi:10.1038/srep13863

Gibson DA, McInnes KJ, Critchley HO, Saunders PT (2013) Endometrial Intracrinology—generation of an estrogen-dominated microenvironment in the secretory phase of women. J Clin Endocrinol Metab 98(11):E1802–1806

Gibson DA, Greaves E, Critchley HO, Saunders PT (2015) Estrogen-dependent regulation of human uterine natural killer cells promotes vascular remodelling via secretion of CCL2. Hum Reprod 30(6):1290–1301

Greaves E, Collins F, Critchley HO, Saunders PT (2013) ERβ-dependent effects on uterine endothelial cells are cell specific and mediated via Sp1. Hum Reprod 28(9):2490–2501

Greca CP, Abrahamsohn PA, Zorn TM (1998) Ultrastructural cytochemical study of proteoglycans in the endometrium of pregnant mice using cationic dyes. Tissue Cell 30(3):304–311

Guo B, Wang W, Li SJ, Han YS, Zhang L, Zhang XM, Liu JX, Yue ZP (2012) Differential expression and regulation of angiopoietin-2 in mouse uterus during preimplantation period. Anat Rec 295(2):338–346

Henderson TA, Saunders PT, Moffett-King A, Groome NP, Critchley HO (2003) Steroid receptor expression in uterine natural killer cells. J Clin Endocrinol Metab 88:440–449

Herington JL, Bany BM (2007) Effect of the conceptus on uterine natural killer cell numbers and function in the mouse uterus during decidualization. Biol Reprod 76(4):579–588

Heryanto B, Rogers PA (2002) Regulation of endometrial endothelial cell proliferation by oestrogen and progesterone in the ovariectomized mouse. Reprod 123(1):107–113

Hewitt SC, Deroo BJ, Hansen K, Collins J, Grissom S, Afshari CA, Korach KS (2003) Estrogen receptor-dependent genomic responses in the uterus mirror the biphasic physiological response to estrogen. Mol Endocrinol 17(10):2070–2083

Hewitt SC, Li L, Grimm SA, Chen Y, Liu L, Li Y, Bushel PR, Fargo D, Korach KS (2012) Research resource: whole-genome estrogen receptor α binding in mouse uterine tissue revealed by ChIP-seq. Mol Endocrinol 26(5):887–898

Kleinfeld RG, O'Shea JD (1983) Spatial and temporal patterns of eoxyribonucleic acid synthesis and mitosis in the endometrial stroma during decidualization in the pseudopregnant rat. Biol Reprod 28(3):691–702

Lindberg MK, Weihua Z, ersson N et al (2002) Estrogen receptor specificity for the effects of estrogen in ovariectomized mice. J Endocrinol 174(2):167–178

Ma WG, Song H, Das SK, Paria BC, Dey SK (2003) Estrogen is a critical determinant that specifies the duration of the window of uterine receptivity for implantation. Proc Natl Acad Sci USA 100(5):2963–2968

Martel D, Psychoyos A (1981) Estrogen receptors in the nidatory sites of the rat endometrium. Science 211:1454–1455

Moggs JG, Tinwell H, Spurway T (2004) Phenotypic anchoring of gene expression changes during estrogen-induced uterine growth. Environ Health Perspect 112(16):1589–1606

Moulton BC, Koenig BB (1981) Estrogen receptor in deciduoma cells separated by velocity sedimentation. Endocrinology 108:484–488

Oliveira SF, Abrahamsohn PA, Nagata T, Zorn TMT (1995) Incorporation of 3H-amino acids by endometrial estromal cells during decidualization in the mouse. A radioautographical study. Cell Mol Biol 42(1):107–116

Oliveira SF, Abrahamsohn PA, Zorn TMT (1998) Radioautography revels regional metabolic differences in the pregnant endometrium of the mice. Braz J Biol Med Res 31(2):307–312

Oliveira SF, Greca CP, Abrahamsohn PA, Reis MG, Zorn TM (2000) Organization of desmin-containing intermediate filaments during differentiation of mouse decidual cells. Histochem Cell Biol 113(4):319–327

Paffaro VA, Bizinotto MC, Joazeiro PP, Yamada AT (2003) Subset classification of mouse uterine natural killer cells by DBA lectin reactivity. Placenta 24(5):479–488

Perrot-Applanat M, Deng M, Fernandez H, Lelaidier C, Meduri G, Bouchard P (1994) Immunohistochemical localization of estradiol and progesterone receptors in human uterus throughout pregnancy: expression in endometrial blood vessels. J Clin Endocrinol Metab 78(1):216–224

Salgado RM, Favaro RR, Martin SS, Zorn TM (2009a) The estrous cycle modulates small leucine-rich proteoglycans expression in mouse uterine tissues. Anat Rec 292(1):138–153

Salgado RM, Capelo LP, Favaro RR, Glazier JD, Aplin JD, Zorn TM (2009b) Hormone-regulated expression and distribution of versican in mouse uterine tissues. Reprod Biol Endocrinol 7:60

Salgado RM, Favaro RR, Zorn TMT (2011) Modulation of small leucine-rich proteoglycans (SLRPs) expression in the mouse uterus by estradiol and progesterone. Reprod Biol Endocrinol 9:22

Salgado RM, Covarrubias AC, Favaro RR, Serrano-Nascimento C, Nunes MT, Zorn TM (2013) Estradiol induces transcriptional and posttranscriptional modifications in versican expression in the mouse uterus. J Mol Histol 44:221–229

Sartor P (1977) Exogenous hormone uptake and retention in the rat uterus at the time of ova-implantation. Acta Endocrinol 84:804–812

Stumpf WE (1968) Subcellular distribution of 3H-estradiol in rat uterus by quantitative autoradiography—a comparison between 3H-estradiol and 3H-norethynodrel. Endocrinology 83(4):777–782

Stumpf WE (1971) Autoradioautographic techniques for the localization of hormones and drugs at the cellular and subcellular levels. Acta Endocr 153:205–222

Stumpf WE (1999) Localizing estradiol and other diffusible hormones and drugs by autoradiography and immunocytochemistry. Histochem Cell Biol 111:83–84

Stumpf WE (2003) Drug localization in tissues and cells. NC7 IDDC-Press, Chapel Hill

Stumpf WE (2012) Drugs in the brain-cellular imaging with receptor microscopic autoradiography. Prog Histochem Cytochem 47(1):1–26

Stumpf WE, Roth LJ (1966) High resolution autoradiography with dry mounted, freeze-dried frozen sections. Comparative study of six methods using two diffusible compounds 3H-estradiol and 3H-mesobilirubinogen. J Histochem Cytochem 14(3):274–287

Stumpf WE, Sar M, Zuber TJ, Soini E, Tuohimaa P (1981) Quantitative assessment of steroid hormone binding sites by thaw-mount autoradiography. J Histochem Cytochem 29:201–206

Tan J, Paria BC, Dey SK, Das SK (1999) Differential uterine expression of estrogen and progesterone receptors correlates with uterine preparation for implantation and decidualization in the mouse. Endocrinology 140(11):5310–5321

Tessier C, Deb S, Prignent-Tessier A, Ferguson-Gottschall S, Gibori GB, Shiu RPC, Gibori G (2000) Estrogen receptors alfa and beta in rat decidual cells: cell-specific expression and differential regulation by steroid hormones and prolactin. Endocrinology 141(10):3842–3851

Tibbetts T, Mendoza-Meneses M, O'Malley B, Conneely O (1998) Mutual and intercompartmental regulation of estrogen receptor and progesterone receptor expression in the mouse uterus. Biol Reprod 59:1143–1152

Wada-Hiraike O, Hiraike H, Okinaga H et al (2006) Role o f estrogen receptor beta in uterine stroma and epithelium: Insights from estrogen receptor beta$^{-/-}$ mice. Proc Natl Acad Sci USA 103(48):18350–18355

Walter LM, Rogers PAW, Girling JE (2005) The role of progesterone in endometrial angiogenesis in pregnant and ovariectomised mice. Reproduction 129(6):765–777

Walter LM, Rogers PA, Girling JE (2010) Vascular endothelial growth factor-A isoform and (co)receptor expression are differentially regulated by 17beta-oestradiol in the ovariectomized mouse uterus. Reproduction 140(2):331–341

Ward WF, Frost AG, Orsini MW (1978) Estrogen binding by embryonic and interembryonic segments of the rat uterus prior to implantation. Biol Reprod 18(4):598–601

Wu Q, Chambliss K, Umetani M, Mineo C, Shaul PW (2011) Non-nuclear estrogen receptor signaling in the endothelium. J Biol Chem 286(17):14737–14743

Zorn TMT, Pinhal MAS, Nader HB, Carvalho JJ, Abrahamsohn PA, Dietrich CP (1995) Biosynthesis of glycosaminoglycans in the endometrium during the initial stages of pregnancy of the mouse. Cell Mol Biol 41:97–106

Zorn TMT, Soto-Suazo M, Pellegrini CR, Oliveira JG, Stumpf WE (2003) Estradiol receptor binding to the epithelium of uterine lumen and glands: region- and time-related changes during pre-implantation and periimplantation periods studied by autoradiography. Histochem Cell Biol 120:1–12